01 Aug 2023

Effect Of Competitive Adsorption Between Specialty Admixtures And Superplasticizer On Structural Build-up And Hardened Property Of Mortar Phase Of Ultra-high-performance Concrete

Le Teng

Jingjie Wei

Kamal Khayat
Missouri University of Science and Technology, khayatk@mst.edu

Joseph J. Assaad

Recommended Citation

L. Teng et al., "Effect Of Competitive Adsorption Between Specialty Admixtures And Superplasticizer On Structural Build-up And Hardened Property Of Mortar Phase Of Ultra-high-performance Concrete," *Cement and Concrete Composites*, vol. 141, article no. 105130, Elsevier, Aug 2023.
The definitive version is available at https://doi.org/10.1016/j.cemconcomp.2023.105130

Cement and Concrete Composites 141 (2023) 105130

Contents lists available at ScienceDirect

Cement and Concrete Composites

journal homepage: www.elsevier.com/locate/cemconcomp

Effect of competitive adsorption between specialty admixtures and superplasticizer on structural build-up and hardened property of mortar phase of ultra-high-performance concrete

Le Teng [a,b], Jingjie Wei [b], Kamal H. Khayat [b,*], Joseph J. Assaad [c]

[a] School of Materials Science and Engineering, Southeast University, Nanjing, Jiangsu, China
[b] Department of Civil, Architectural and Environmental Engineering, Missouri University of Science and Technology, Rolla, MO, USA
[c] Department of Civil and Environmental Engineering, University of Balamand, Al Kourah, PO Box 100, Lebanon

ARTICLE INFO

Keywords:
Competitive adsorption
Latex polymer
Structural build-up
Ultra-high-performance concrete
Viscosity modifying admixture

ABSTRACT

This study aims to enhance structural build-up of ultra-high-performance concrete (UHPC) without influencing the initial flowability, which is critical in repair applications (e.g., use of UHPC in thin bonded overlays for bridge deck rehabilitation). Specialty admixtures, such as a viscosity-modifying admixture (VMA), have been used to enhance the structural build-up at rest. However, the use of specialty admixtures can increase superplasticizer (SP) demand to maintain proper flowability; the synergistic effect of these admixtures on structural build-up is not well understood as the coupled admixture content can reverse the net effect on yield stress, viscosity, and thixotropy. In this study, VMAs including welan gum (WG), diutan gum (DG), and cellulose ether (CE) were used. Styrene-butadiene rubber (SBR) and acrylic ester (AE) latex polymers (LPs) that can enhance structural build-up and bond strength were also incorporated. The competitive adsorption between these specialty admixtures and SP and its effect on structural build-up, early-age hydration, compressive and pull-off strengths, porosity and entrapped air content of UHPC mortar (i.e., without fiber) were systematically investigated. Test results indicated that the incorporation of anionic WG and DG that exhibited high competitive adsorption with SP led to a 275%–450% enhancement in structural build-up despite the 55%–135% increase of SP demand. Such increase was limited to 130% when using CE, SBR, or AE that cannot effectively adsorb onto cement particles in the presence of SP. This was because the high competitive adsorption between specialty admixtures and SP strengthened the particle flocculation and promoted the cement hydration in the first hour; the latter resulted in 20%–40% enhancement in non-reversible component of structural build-up. Furthermore, the use of LP at low and moderate dosages secured high bond strength to normal strength mortar despite 8%–33% decrease in compressive strength given the increased capillary porosity. The use of VMAs increased the entrapped air and resulting 5%–15% lower compressive strength, while the bond strength was not influenced.

1. Introduction

Ultra-high-performance concrete (UHPC) is an advanced fiber reinforced composite material with high mechanical properties and durability [1–3]. The conventional UHPC has high apparent viscosity due to the low water-to-binder ratio (w/b) and the incorporation of high volume of fine powders (e.g., silica fume) [3,4], which can lead to difficulty in mixing, casting and placing. The use of supplementary cementitious materials (e.g., fly ash and slag) and improved sand gradation to increase packing density and polycarboxylate ether superplasticizer (SP) to reduce the water demand can design the self-consolidating UHPC that exhibits low yield stress and plastic viscosity in the order of 10–30 Pa and 20–50 Pa s, respectively [4], which can facilitate casting [5,6]. While suitable for many structural applications, self-consolidating UHPC can present special challenges when used for the rehabilitation of bridge decks where a highly flowable material can sag during placement on sloped substrates and fibers or coarse aggregate may segregate [7,8]. Self-consolidating concrete can also exert high lateral pressure on vertical formwork when retrofitting the relatively tall structures, such as columns and bridge piers [9,10]. Earlier studies showed that such limitations can be rectified by tailoring the rheological properties to either secure a moderate yield stress values [8] or to develop a high structural build-up at rest [9,11,12]. Latter reflects the increase of yield stress and

* Corresponding author.
E-mail address: khayatk@mst.edu (K.H. Khayat).

https://doi.org/10.1016/j.cemconcomp.2023.105130
Received 25 January 2023; Received in revised form 10 April 2023; Accepted 11 May 2023
Available online 12 May 2023

Nomenclature

τ_d	dynamic yield stress (Pa)
A_{sb}	increasing rate of static yield stress from 5 to 30 min (Pa/min)
$A_{\tau d}$	increasing rate of dynamic yield stress after end of mixing (Pa/min)
h	height of the coaxial cylinder submerged in the materials (m)
μ	plastic viscosity (Pa • s)
τ_s	static yield stress (Pa)
T	torque (N·m)
T_{max}	maximum torque (N·m)
G	intercept of the flow curve (N·m)
R_o	radius of rheometer container (m)
D_g	gap size of rheometer (m)
Ω	volume of mini-slump cone (m^3)
N	rotational velocity (m/s)
H	slope of the flow curve (N·m/s)
R_i	radius of coaxial cylinder (m)
ρ	density of UHPC mortar (kg/m^3)
R_f	radius of mini-slump spread (m)

Abbreviation

VMA	viscosity-modifying admixture
CE	cellulose ether
DG	diutan gum
AE	acrylic ester
LP	latex polymer
WG	welan gum
SBR	styrene-butadiene rubber
SP	superplasticizer

viscosity with rest time [9–11].

The structural build-up is influenced by the physical structuration and chemical rigidification. Particle colloidal flocculation after removing shear stress is the origin of physical structuration of cementitious materials [13]. It is affected by the number of particle contacts that depend on the particle volume fraction and maximum packing density [14,15], and the colloidal surface attraction between adjacent fine particles that influenced by type of chemical admixtures and surface coverage by those admixtures [16,17]. On the other hand, the cement hydration can lead to chemical rigidification (e.g., stable C–S–H) that can increase the structural build-up [18–20]. In general, the variation of the water-to-cementitious materials ratio (w/cm) [21,22], cementitious materials content and type [23,24], as well as the use of nanomaterials [25,26] and chemical admixtures [27–31] can change the particle colloidal flocculation, resulting in different levels of structural build-up.

UHPC with high fluidity can exhibit a relatively low structural build-up due to the high SP content [10,30]. Previous studies show that the structural build-up can be greatly improved by incorporating viscosity-modifying admixtures (VMAs) without altering mixture proportion (i.e., w/b and cementitious materials), which can secure limited variation of hardened properties of UHPC [30,31]. For instance, the increase of welan gum content from 0 to 0.09%, by mass of biner, was found to enhance static yield stress of UHPC mortar from 12 to 41 Pa/min [30]. The impact of VMA on enhancing structural build-up is dependent on the VMA type. Cui et al. [32] proposed that the use of hydroxypropyl methyl cellulose can be more effective to increasing structural build-up of UHPC compared to polyacrylic acid or welan gum. The incorporation of VMA can increase SP demand, thus reducing the overall effectiveness of the VMA on thixotropy due to the greater steric repulsive forces [27,28]. Khayat and Assaad [12] used the breakdown area to evaluate the influence of cellulosed-based VMAs on the structural build-up of self-consolidating concrete prepared with various SP dosages. The results showed that the breakdown area can decrease from 21% to 9% when the VMA is further increased from 260 to 730 mL/100 kg of cementitious materials, given the need for more SP to maintain a slump flow of 650 mm [12].

The incorporation of latex polymer (LP) can also increase the structural build-up given the formation of polymer network [33–35]. The common latex polymers used in cement-based materials include styrene-butadiene rubber (SBR) and acrylic ester (AE). Assaad [33] reported that the increase of AE content from 0% to 20% was shown to increase the structural breakdown area by 400%. It is also worth to mention that the use of LP can enhance the bond strength to existing concrete, which is important for UHPC with relatively high structural build-up that can be particularly vulnerable to bond losses to existing concrete substrates [36]. Graybeal and Haber [36] reported that the bond strength between thixotropic UHPC and conventional concrete was 0.8 MPa when the diamond grinding was used to prepare the surface. Yet, the bond increased to 1.8 MPa when the latex-modified concrete was used as the overlay material, reflecting the relevance of LP to secure a monolithic behavior of the overlay-substrate composite structure [37,38]. The pull-off bond strength between polymer-modified high strength grout and conventional concrete was investigated in Ref. [33]. Results show that the use of 20% styrene-butadiene rubber (SBR) or acrylic ester (AE), by volume of water, changed the mode of failure (i.e., from interface to cohesive within the substrate), reflecting enhanced bond strengths.

Limited studies investigated the synergistic influence of specialty admixtures (i.e., VMAs and LPs) and SP on structural build-up of UHPC made with a constant fluidity (i.e., SP dosage varied with the addition of specialty admixtures). The mechanism behind the variation of structural build-up in such systems is not well understood, especially knowing the presence of competitive adsorption between specialty admixtures and SP; high SP dosage can reduce or reverse the benefit of the specialty admixtures on structural build-up. Furthermore, the combined specialty admixtures and SP can impact bond strength between thixotropic UHPC and conventional concrete substrate, which is a key property in thin bonded UHPC rehabilitation projects. This study investigates the competitive adsorption between SP and specialty admixtures, including welan gum, diutan gum, and cellulose ether VMAs as well as styrene-butadiene rubber and acrylic ester LPs. The effect of the competitive adsorption between specialty admixtures and SP on dynamic yield stress, plastic viscosity, structural build-up, and early-age hydration of the non-fibrous UHPC mortar was then studied. Each specialty admixture was used at three or four contents combined with various SP dosages to maintain the mini-slump flow at 200 ± 10 mm. This studies also determines the coupled influence of these admixtures and SP on the compressive strength, pull-off strength, and pore structure of the UHPC matrix.

2. Mixture proportions and sample preparation

2.1. Chemical admixtures

A polycarboxylate-based SP complying with ASTM C494 Type F was employed in this work; its specific gravity at 20 °C and solid content were 1.05 and 26%, respectively. A polyether-based air detraining admixture was used in all mixtures at fixed rate of 0.04%, by binder mass, to reduce air entrainment and influence on porosimetry measurements. Its specific gravity and solid content were 1.01 and 5%, respectively.

Three types of VMAs were used to enhance structural build-up of

investigated UHPC including a cellulose ether (CE) polymer in liquid form along with a welan gum (WG) and diutan gum (DG) in powder form. The CE is chloride-free and complies to ASTM C494 Type S; its solid content is 30%. According to the manufacturer's Technical Data Sheet, a slight decrease in slump and increase in air content may be encountered when using the CE admixture. The WG and DG are microbial high-molecular weight polysaccharides used as rheology-modifiers or structural build-up modifiers in numerous industrial applications. As shown in Fig. 1, the WG molecule is made of repeating tetrasaccharide chains with single L-mannose or L-rhamnose branches, while the DG backbone consists of similar branches along with D-glucose side chain monomers [39]. The WG and DG are compatible with the cement hydration since they are stable in high potential of hydrogen (PH) systems [40]; their average molecular weights are between 4.1 and 5.2 million Da, and their bulk densities are approximately 410 kg/m^3.

This study also employed the SBR latex and AE latex that are both dispersions of latex particles in water with slight negative stabilization. The molecular structures of SBR latex and AE latex are presented in Fig. 1(b). The SBR and AE solid contents are 48% and 24%, respectively, and they have the same specific density of 1.01. No incompatibility (such as abnormal loss in workability and excessive delay in setting) was noticed between the polycarboxylate-based SP and various VMAs and LPs used in this study.

2.2. UHPC mixture proportions

A non-proprietary UHPC with w/b of 0.2 designed in compliance with the rheology-based method was used in this study [41]. The binder system contained 55% Type III cement, 5% unidentified silica fume, and 40% Class C fly ash. Such binder system was found to reduce considerably the SP demand, improve the packing density of the binder, and mitigate the autogenous shrinkage [41]. The sand consisted of 30% fine masonry sand, 53% concrete river sand, and 17% saturated lightweight sand determined using the modified Andreasen and Andersen model for particle packing. The binder-to-sand ratio was set at 1.0 that proved to increase compressive strength [41]. The physical properties and particle size distribution of the raw materials are presented in Table 1 and Fig. 2, respectively.

Different structural build-up levels were secured by adding the VMAs and LPs at low, moderate, and high concentrations based on the Materials' specifications recommended by the admixture producers. For example, the powdered DG is typically recommended up to 0.02% of the binder mass, while the contents could reach 0.5% for the WG. The active materials in the liquid CE admixture are recommended to vary between 0.2% and 1.5% of the binder mass. The preliminary results realized in this testing program have shown that the SP demand will excessively increase to maintain the needed flow, which would increase air entrainment in the fresh UHPC and significantly delay the setting times.

In the case of the LPs (i.e., SBR and AE), the low, moderate, and high concentrations recommended by the admixture manufacturers were used. The maximum dosages were mainly determined based on the drop in compressive strength, given the detrimental effects of such latexes on the compression properties of cementitious materials [37]. Special care was placed to maintain the w/b constant at 0.2 by accounting the amount of water existing in such LPs, and a threshold drop of 25% in compressive strength was tolerated in this testing program. In total, 18 mixtures were investigated, as presented in Table 2.

2.3. Mixing, casting, and curing procedures

Raw materials were mixed at room temperature. A magnetic stirrer was employed to disperse the WG and DG powder with 90% of the SP for 10 min at 15 rps to secure uniform dispersion before batching. The WG and DG solutions were then added into 90% of the mixing water. The CE, SBR, and AE were added along with 90% of the mixing water and SP before batching. A 19-L Hobart mixer was used to prepare the UHPC mortar. The mixing procedure was as follows: (1) the dry materials were mixed for 2 min at 1 rps; (2) the pre-prepared solution of chemical admixtures was added and mixed for 3 min at 2 rps; and (3) the remaining 10% of the mixing water and SP was added and mixed for 7 min at 2 rps. The temperature of mixing water was adjusted to secure that the temperature of UHPC was at 20 ± 2 °C at the end of mixing.

The samples to determine the hardened properties of investigated UHPC mortars were cast in one lift followed by slight mechanical consolidation. The specimens were covered using wet burlap and plastic sheet. After one day, these specimens were demolded and cured using lime-saturated water at 20 ± 2 °C during the first 3 days. They were then sealed in the polyethylene bags and stored in curing room where the temperature was 20 ± 2 °C and relatively humidity was greater than 90% until the time of testing. This curing protocol can avoid the destabilization of the polymer LP films due to the complete soaking of specimens in water [37]. Nevertheless, the proposed curing protocol is different from the continuous moist curing reported by ASTM 1856. It is worth noting that the reference UHPC was subjected to two different curing methods including the proposed one as well as by exposing it to continuous moist curing as reported in ASTM C1856.

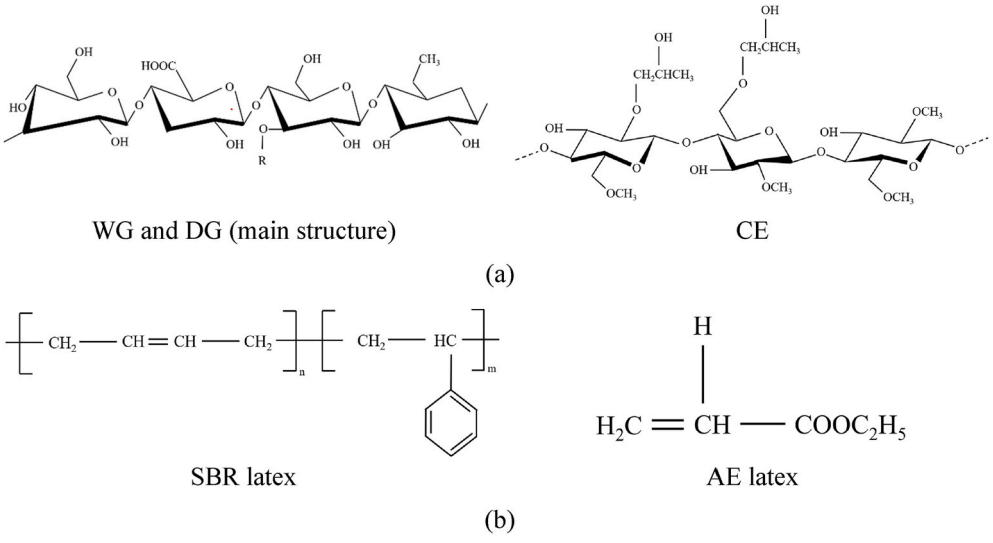

Fig. 1. Molecular structure of: (a) VMA; and (b) LP.

Table 1
Physical properties of the cementitious materials and sands used in UHPC.

	Type III Cement	Silica fume	Class C fly ash	River sand	Lightweight sand	Masonry sand
Specific gravity	3.15	2.20	2.70	2.65	1.81	2.64
B.E.T. (m^2/kg)	–	18,200	–	–	–	–
Blaine surface area (m^2/kg)	560	–	465	–	–	–
D_{max} (mm)	–	–	–	4.75	4.75	2
D_{50} (mm)	0.01	0.0035	0.012	0.65	2.3	0.35
Water absorption (%)	–	–	–	1.4	17.6	1.6

Note: D_{max} (mm) is the maximum particle diameter; and D_{50} (mm) is the mean particle diameter.

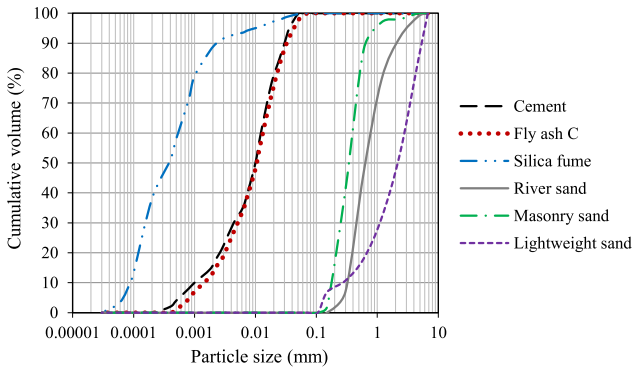

Fig. 2. Particle size distribution of the binder and sand.

3. Test methods

3.1. Rheology

3.1.1. Bingham properties

A Contec 5 coaxial cylinder rheometer was used to determine the rheology of UHPC mortars, as shown in Fig. 3. Each mixture was replicated three times to assess the repeatability of results, and the mean values were considered for analysis. The Bingham properties were measured right after the end of mixing (i.e., time interval for transferring the material from the mixer to the rheometer was within 1 min). The UHPC mortar mixtures were pre-sheared using 0.5 rps for 30 s, then the impeller rotational velocity gradually decreased from 0.5 to 0.025 rps in 10 steps. During each step, 25 data points were collected. The dynamic yield stress (τ_d) and plastic viscosity (μ) were calculated using the Bingham model, as shown in Eqs. (1)–(3). Data points at rotational velocities of 0.5 and 0.45 rps were removed given the lack of equilibrium [42].

The same test procedure was also used to determine the Bingham properties at 5, 15, and 30 min for the reference UHPC mortar and the mixtures containing VMA and LP at contents that displayed the highest structural build-up. The increase of dynamic yield stress with time is mainly due to the chemical rigidification, which is important to understand the mechanism of using VMA and LP to increase the structural build-up of UHPC. The mortar samples were placed in the Hobart mixer and covered using wet towel and plastic sheet in the rest period. Then, they were re-agitated at 3 rps using Hobart mixer for 120 s before each

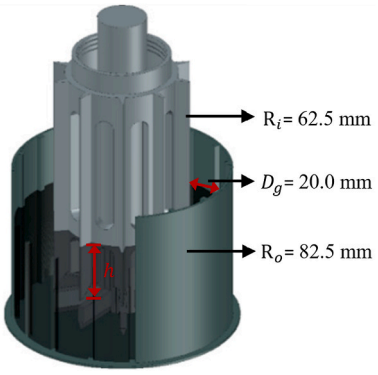

Fig. 3. Schematic diagram of the Contec 5 rheometer (unit: mm).

Table 2
Mixture proportion of investigated UHPC mortars.

Mixture	Type III Cement	Silica fume	Fly ash C	River sand	Lightweight sand	Masonry sand	CE	WG	DG	SBR[a]	AE[a]
	(kg/m^3)						(%-by mass of cementitious materials)				
Ref	649	41	405	516	118	302	–	–	–	–	–
CE-0.25							0.25	–	–	–	–
CE-0.5							0.5	–	–	–	–
CE-1							1	–	–	–	–
CE-1.5							1.5	–	–	–	–
WG-0.09							–	0.09	–	–	–
WG-0.18							–	0.18	–	–	–
WG-0.27							–	0.27	–	–	–
DG-0.0015							–	–	0.0015	–	–
DG-0.003							–	–	0.003	–	–
DG-0.0075							–	–	0.0075	–	–
DG-0.015							–	–	0.015	–	–
SBR-0.45							–	–	–	0.45	–
SBR-0.9							–	–	–	0.9	–
SBR-1.8							–	–	–	1.8	–
AE-0.23							–	–	–	–	0.23
AE-0.45							–	–	–	–	0.45
AE-0.9							–	–	–	–	0.9

Note.
[a] Refers to active portion.

test to secure the structural breakdown. It should be mentioned that the materials were not re-agitated using rheometer to avoid the effect of plug flow. Typical results of the reference UHPC are shown in Fig. 4(a). Fig. 4(b) shows the τ_d linearly increased with rest time for the reference mixture. Similar trends were found for other mortars containing VMAs and LPs. The slope of the curve ($A_{\tau d}$) refers to the increase rate of dynamic yield stress, which was used to compare with the increase rate of static yield stress to underline the action mode of VMA and LP in UHPC mixture.

$$T = G + H \cdot N \tag{1}$$

$$\tau_d = \frac{\left(\frac{1}{R_i^2} - \frac{1}{R_o^2}\right)}{4\pi h \, ln\left(\frac{R_o}{R_i}\right)} G \tag{2}$$

$$\mu = \frac{\left(\frac{1}{R_i^2} - \frac{1}{R_0^2}\right)}{8\pi^2 h} H \tag{3}$$

where T (N·m) is the torque, G (N·m) is the intercept of the flow curves, H (N·m/s) is the slope of the flow curves, N (m/s) is the rotational velocity, h (m) is the height of the inner cylinder submerged in the materials tested in the rheometer, R_i (m) is the radius of coaxial cylinder (R_i = 0.0625 m), and R_o (m) is the radius of the container (R_o = 0.0825 m).

3.1.2. Static yield stress and assessment of structural build-up

The structural build-up at rest was determined using the development of the static yield stress (τ_s) after 5-, 15-, and 30-min rest periods. The mortar was subjected to a low rotational velocity of 0.05 rps for 120 s during each test, which then the sample is stirred to reduce the formation of preferential planes due to particle orientation and kept undisturbed during the rest period [12]. As typically shown in Fig. 5(a), the resulting torque of the reference UHPC mortar was progressively increased with time to a peak value before flow occurrence. The τ_s is calculated using Eq. (4) [43], Fig. 5(b) presents the variation of τ_s value of the reference mixture with time where a rapid increase occurred at first 5 min followed by a linear increase with time. Similar trends were found for other UHPC mortars containing VMAs and LPs., This study used the increasing rate of τ_s from 5 to 30 min (A_{sb}) to assess the structural build-up in compliance with [31,44].

$$\tau_s = \frac{T_{max}}{2\pi h R_i^2} \tag{4}$$

where T_{max} (N·m) corresponds to the peak of torque in the testing process.

3.2. Compressive strength and modified pull-off test

The 28-d compressive strength of UHPC mortar was tested using 50-mm cubes based on ASTM C109; the loading rate was 5 kN/min. The bond strength between UHPC and normal strength mortar (NSM) was determined using dogbone composite samples, as shown in Fig. 6. The mixture proportion of NSM is based on conventional concrete reported in Ref. [45] after the removal of aggregates larger than 4.75 mm by sieving the concrete mixture. A plastic clip was used to divide the dogbone sample into two parts. NSM was cast in the half of the molds. The sand-blasted surface of NSM was prepared to enhance the bond strength; this was achieved by spraying retarder on the surface of plastic clip to enable the removal of surface paste of NSM after demolding. The NSM was then cured in lime-saturated water at 20 ± 2 °C for 28 days. Then, the NSM was placed into the molds followed by casting UHPC into the other half part. The composite dogbone specimens were subjected to a pull-off tensile loading at a rate of 0.1 mm/min. Three specimens were measured for compressive strength and modified pull-off tests for each mixture.

3.3. Heat of hydration

Hydration kinetics were evaluated using an isothermal conduction calorimetry. Approximately 60 g of fresh UHPC mortar was placed and sealed into the calorimetry immediately after end of mixing. The test temperature and duration were set at 20 °C and 48 h, respectively.

3.4. Zeta potential test

The zeta potential test was conducted using the Malvern Zetasizer Nano to evaluate the adsorption of VMA, LP, and SP onto the cement particles. Generally, the total organic carbon test is used to investigate the adsorption of chemical admixtures onto the cement particles [46]. However, the authors found that it was difficult to centrifuge the water due to the low w/b when conducting total organic carbon test. Previous studies reported that the zeta potential results of cement paste made with SP and various macromolecular admixtures were consistent with the results measured using total organic carbon test [47,48]. Furthermore, the relative adsorption isotherms of the different specialty admixtures in diluted slurries should be similar to that in the actual concentrated slurries [49,50]. Sha et al. [49] investigated the adsorption of four different polycarboxylate superplasticizers onto cement particles using total organic carbon and zeta potential tests. The cement paste made with w/cm of 0.29 was used to conduct the total organic carbon test, whereas the cement slurry prepared with w/cm of 50 was employed for the zeta potential test. Results show that the polycarboxylate

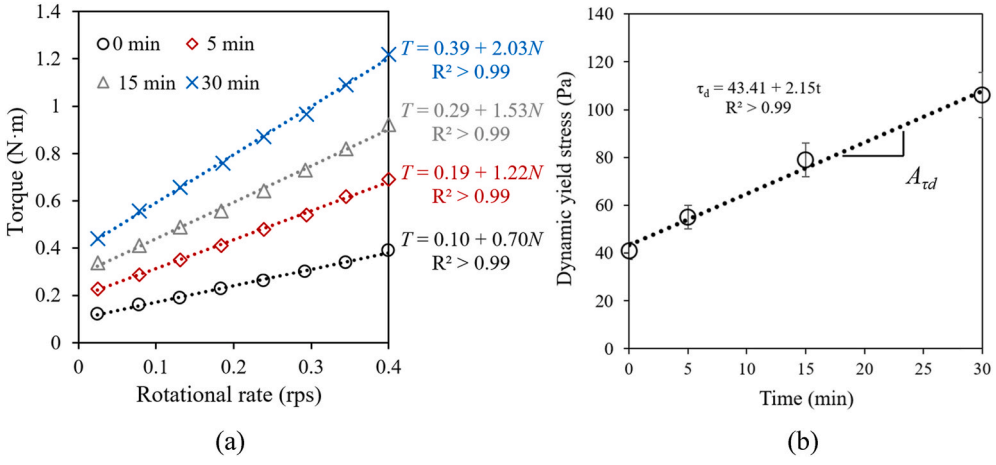

Fig. 4. (a) Flow curves of the reference mixture determined at different resting time; and (b) increase of dynamic yield stress with time of the reference mixture.

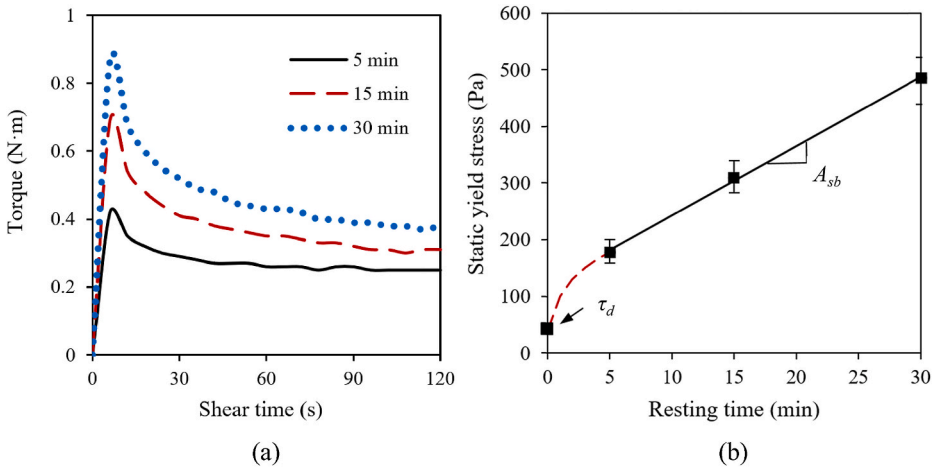

Fig. 5. Variations of: (a) torque with rest time; and (b) static yield stress with rest time for the reference UHPC mortar.

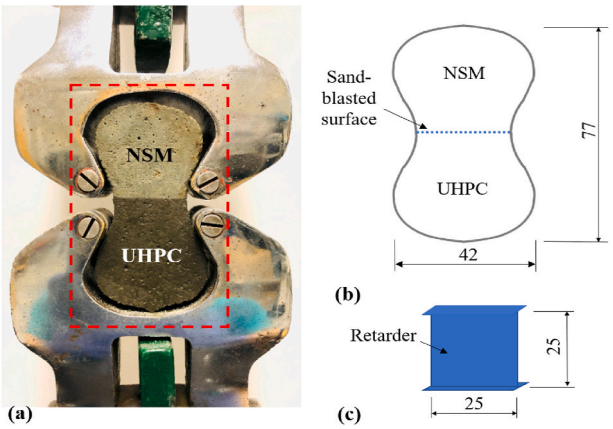

Fig. 6. Methodology of modified pull-off test: (a) test setup; (b) specimen dimensions; and (c) clip dimensions (unit: mm).

superplasticizer that exhibited higher adsorption capacity onto the cement particles led to a lower zeta potential of slurry. Ma et al. [50] stated that the use of VMA that led to a lower zeta potential value of slurry made with w/cm of 40 was more effective to increase the yield stress and plastic viscosity of cement paste made with w/cm of 0.29 due to the higher adsorption capacity. This indicated that the zeta potential in diluted slurry can reflect the adsorption of macromolecules, such as VMA and LP, onto cement particles in actual cement-based based materials. A highly diluted slurry with 1% cement concentration was prepared in compliance with [51]. The composition of cementitious materials is the same to the investigated UHPC mixture. The slurry was prepared as follows: (1) mixing deionized water and chemical admixtures, including SP, VMA, and LP at 700 rpm for 10 min followed by a 10-min high-intensity sonification treatment; and (2) mixing cementitious materials and prepared solutions at 700 rpm for 10 min; The test was conducted at 0, 15, 30, 45, and 60 min after the preparation of diluted slurry, and each slurry mixture was repeated three times to secure the reproducibility of the results. The diluted slurry was constantly mixed at 350 rpm during the test to avoid the segregation of cement particles. The PH value of each diluted slurry was also measured.

3.5. Image analysis for air content

Two slices measuring 100 mm in diameter and 5 mm in thickness were saw-cut from the center of cylinder specimen measuring 100 × 200 mm to determine the air content of UHPC mortar. In total, six slices taken from three specimens were obtained for each mixture. The slices were polished using silicon carbide papers with grit sizes of 80, 180, 360, and 600. In order to contrast the air content from other parts of UHPC, the surface was blackened using the marker followed by pressing white Barium Sulfate powder into the air voids. A high-resolution image of the cross section was photographed and binarized to evaluate the air content in hardened UHPC mortar.

3.6. Mercury intrusion porosimetry

The mercury intrusion porosimetry was employed to determine the porosity of UHPC mortars. Samples measuring 1–1.5 mm were taken from the center of the cylinder specimens at 28 d. These samples were soaked in ethyl alcohol for 24 h to stop further cement hydration followed by drying at 60 °C in a vacuum oven for 48 h. The test pressure ranged between 0.25 and 415 MPa.

4. Experimental results

4.1. Competitive adsorption between specialty admixtures and SP

The mechanism of VMAs and LPs influencing the rheological property of UHPC mortar can correlate to their affinity with the particle surface of cementitious materials. The zeta potential can determine the surface charge at the stern layer of colloidal particle that might be affected by the adsorption of SP, VMAs, and LPs [52]. Fig. 7 presents the variation of zeta potential with time for diluted slurry of UHPC binder made without any admixtures, with 0.1% admixtures only, and with 0.1% admixtures and 0.5% SP. The positive and negative values represent the cation and anion dominated at the surface of stern layer, respectively. The zeta potential of slurry made without any SP was positive and slightly increased with time. This was due to the cationic property of early-age hydration products, such as ettringite [53]. On the other hand, the use of 0.5% SP reduced the zeta potential of the diluted slurry made without any VMA and LP to a negative value due to the adsorption of anionic SP onto the cement particles. Furthermore, the zeta potential value slightly decreased with time and became relatively stable at 30 min.

As shown in Fig. 7(a), the zeta potential values varied from 1.5 to 4 mV for reference diluted slurry. The use of 0.1% WG and DG significantly reduced the zeta potential where the values ranged between −19 and −23.5 mV given the anionic carboxylate group of WG and DG polymers. Such variation of zeta potential value might be due to the anionic WG and DG polymers that remain in the water or the adsorption of WG and DG onto the cement particles that can change the surface charge at the stern layer of the cement particles [32,40,54]. The use of

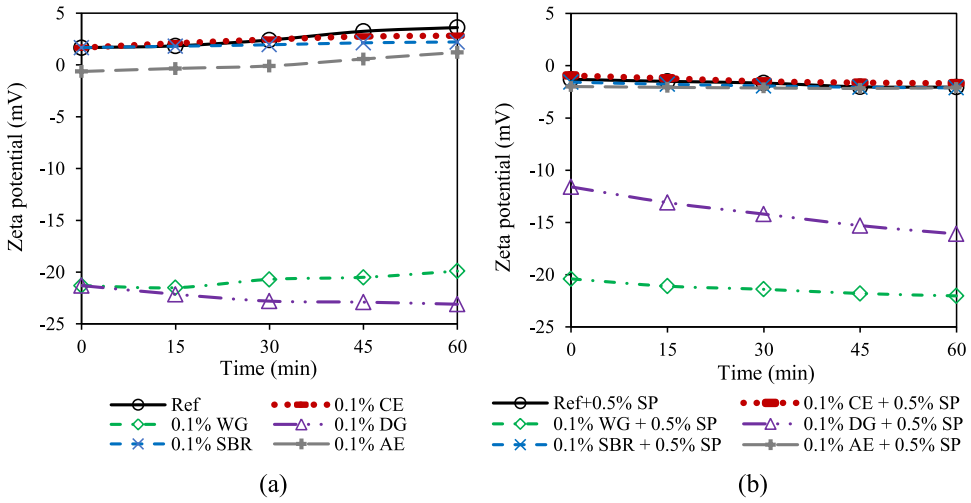

Fig. 7. Variation of zeta potential with time for slurry mixtures made with 0.1% various specialty admixtures and: (a) without any SP; (b) with 0.5% SP.

SP decreased the influence of WG and DG on reduction in zeta potential, as shown in Fig. 7(b). For example, the zeta potential value at 30 min was −13 mV for UHPC made with a combination of 0.1% DG and 0.1% SP, which is higher than −22mV for UHPC prepared with 0.1% DG. If the zeta potential value reflects the anionic WG and DG remaining in the water, the incorporation of SP cannot increase the zeta potential given the adsorption of the SP onto cement particles [46,53]. Furthermore, the carboxylic acid group of SP can decrease the zeta potential even though the SP cannot adsorb onto the cement particles [51]. Therefore, the adsorption of WG and DG onto the cement particles is the origin of the variation of the zeta potential. The competitive adsorption between SP and WG or SP and DG can decrease adsorption of WG and DG onto the cement particles, resulting in a less reduction in zeta potential values. On the other hand, the diluted slurry made with 0.1% CE, SBR, and AE exhibited a similar zeta potential compared to the reference slurry, especially after the incorporation of SP. This limited variation in zeta potential can be attributed to: (1) limited adsorption of polymers onto the cement particles [55]; and (2) the adsorption of non-ionic polymers cannot change the zeta potential [40].

The impact of VMA and LP content on the zeta potential of slurry at 30 min is plotted in Fig. 8. The increase of WG content from 0 to 0.3% and DG content from 0 to 0.1% greatly reduced the zeta potential from approximately 2.5 to −22.5 mV. Further increase in WG and DG contents had a limited influence on the zeta potential. Therefore, the 0.3% of WG and 0.1% of DG content can be considered as saturation content

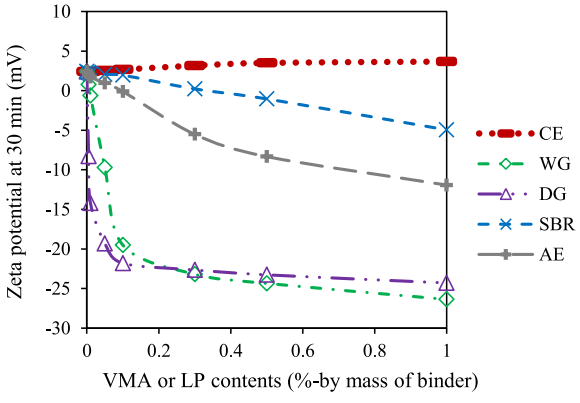

Fig. 8. Effect of specialty admixture contents on zeta potential of slurry made without any SP at 30 min.

for the investigated UHPC binders. The zeta potential reduced from approximately 2.5 to −5 mV with the increase of SBR content from 0 to 1%. The use of 1% AE decreased the zeta potential from 2.5 to −11.9 mV. This indicates that the 0.1% is a relatively low dosage compared to the saturation dosage of LPs, which led to a low adsorption and limited variation of zeta potential (Fig. 7). In the case of CE, the zeta potential slightly increased from 2.5 to 3.5 mV with the increase of CE content from 0 to 1%. This reflects that the non-ionic characteristic of the CE cannot change zeta potential even though the CE polymers can adsorb onto the cement particles [40,55,56].

Fig. 9(a) shows that the adsorption of specialty admixtures gradually decreased and the adsorption of SP increased with the addition of SP. This can be reflected by the fact that the zeta potential value of slurry containing specialty admixtures tended to the value of the slurry prepared with only SP when the SP content increased. The zeta potential values of slurry made with 1% SP and 1% CE, SBR or AE exhibited a similar zeta potential value compared to the slurry prepared with 1% SP and without any specialty admixture, indicating that the use of 1% SP can fully desorb the CE, SBR and AE from cement particles [57]. In the case of slurry made with DG and WG, the increase of SP content enhanced the zeta potential value from approximately −21 to −12 mV, which demonstrated that the relative adsorption of WG and DG decreased by 55% when 1% SP was incorporated. The zeta potential of −12 mV of the slurry made with 0.1% WG and DG and 1% SP demonstrated that WG and DG can effectively adsorb onto cement particles even when the SP content was 10 times higher than their contents.

The impact of the specialty admixtures on the SP adsorption for slurry made with 1% SP is presented in Fig. 9(b). The increase of CE, SBR and AE contents had a limited influence on the zeta potential, which demonstrated that the adsorption of SP cannot be greatly affected by incorporating these specialty admixtures. The addition of WG and DG was shown to desorb part of SP given the great reduction of the zeta potential. For instance, the increase of WG content from 0 to 0.1% decreased the zeta potential from −2 to −14 mV. To sum up, the WG and DG had a high competitive adsorption with SP, while the adsorption of CE, SBR and AE was limited in the presence of SP.

4.2. SP demand, dynamic yield stress and plastic viscosity

The effect of VMA and LP on SP demand of UHPC made with mini-slump flow of 200 mm is shown in Fig. 10. The SP demand increased with the use of VMA; for example, the increase of DG content from 0 to 0.015% resulted in 265% higher SP demand. The competitive adsorption onto cement particles between VMA and SP is the main reason to

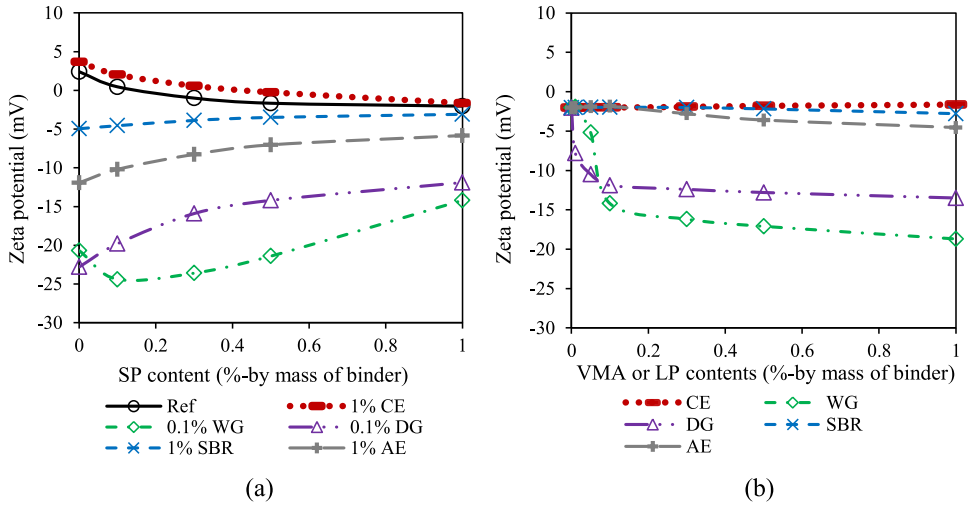

Fig. 9. Variations of zeta potential at 30 min with: (a) SP content for slurry prepared with various specialty admixtures; and (b) VMA or LP contents for slurry made with 1% SP.

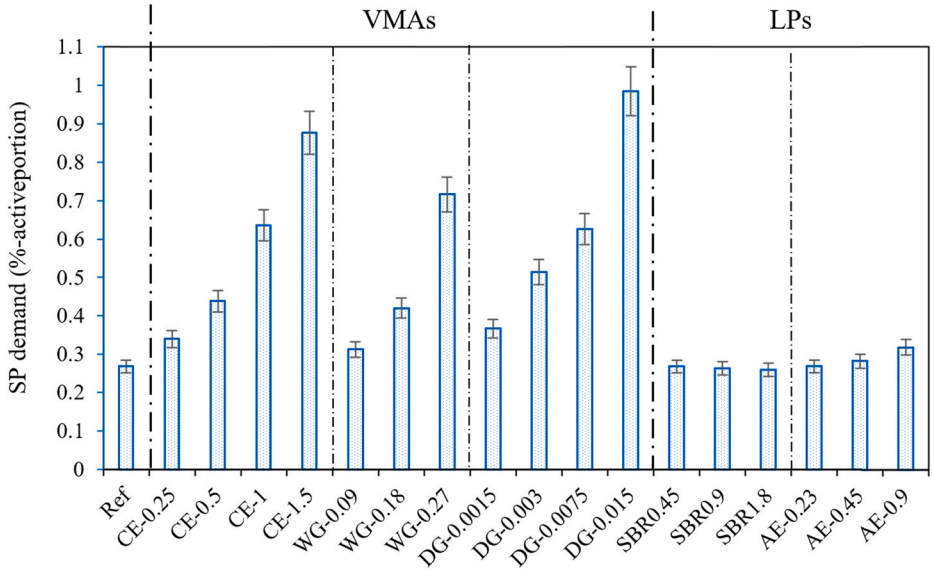

Fig. 10. Influence of using different types and contents of VMA and LP on SP demand for UHPC mortar with a constant mini-slump flow of 200 ± 10 mm.

necessitate additional SP to maintain the required workability, as elaborated in Section 4.1. The other reason is that the long polymer chains of VMA can fix part of the free water, thus resulting in a higher SP demand to disperse the cement particles [58]. The addition of SBR and AE was shown to have a limited influence on SP demand, which was consistent with the results that the addition of SP had a limited effect on SP adsorption.

Fig. 11 presents the variation of dynamic yield stress (τ_d) and plastic viscosity (μ) of UHPC made with combinations of specialty admixtures and SP. The τ_d values varied from 32 to 48 Pa at the end of mixing given the constant flowability (200 ± 10 mm). Such variations in τ_d were consistent with the results determined by Eq. (5) proposed by Roussel [59]; the calculated τ_d ranged between 30 and 45 Pa when the mini-slump flow varied from 190 to 210 mm.

$$\tau_d = \frac{225\rho g \Omega^2}{125\pi^2 R_f^5} \quad (5)$$

where ρ (kg/m^3) is the density of UHPC mortar; g (N/kg) is the gravity, Ω (m^3) is the volume of slump cone, R_f (m) is the radius of mini-slump flow.

The μ was shown to significantly increase with the use of VMA. The use of WG had the greatest effect on increasing the μ value, followed by CE and DG. For example, the increase of WG content from 0 to 0.27% enhanced the μ value from 7 to 59 Pa s. The μ value increased up to 45 Pa s by using 1.5% CE and 31 Pa s by adding 0.0075% DG. The competitive adsorption between VMA and SP can influence μ in two different ways. On one hand, a higher adsorption of SP compared to VMA can enhance the μ value of interstitial pore solution due to the long polymer chain of VMA that can fix part of mixing water and entangle with other adjacent VMAs to form a network in transitional solution [58]. This can increase the μ of interstitial pore solution, which can promote a higher μ value of mortar without affecting the yield stress. On the other hand, the excessive non-adsorbed VMA and SP polymer can form the hydrodynamic lubrication layer to prevent the direct contact between solid particles, which can hinder the effect of VMA on enhancing μ [60]. DG can adsorb onto multiple cement particles due to the high molecular mass and effective competitive adsorption with SP; limited increase of DG content led to a high additional SP demand,

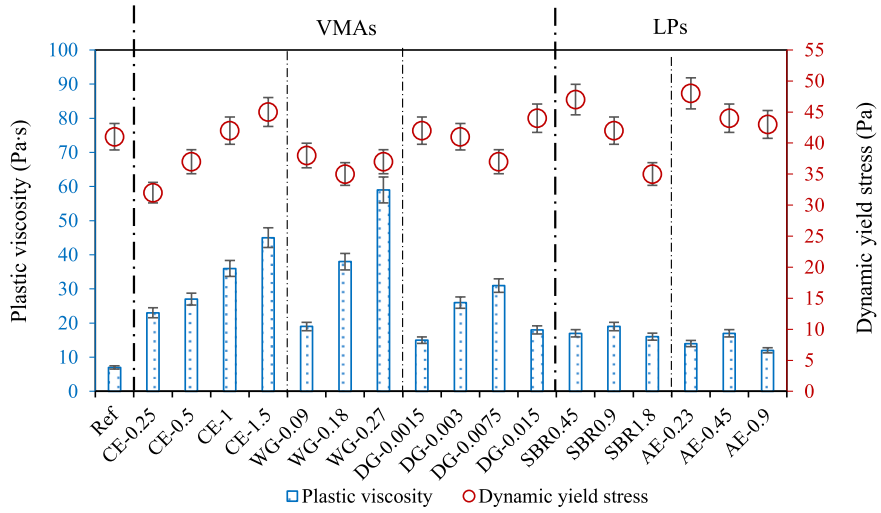

Fig. 11. Effect of competitive adsorption between specialty admixtures and SP on dynamic yield stress and plastic viscosity of UHPC mortar with a constant mini-slump flow of 200 ± 10 mm.

which led to the lowest effect DG on enhancing μ. In the case of CE, the hydrodynamic lubrication effect became nonnegligible due to its low adsorption in the presence of SP, resulting in a lower increase in μ value compared to the WG.

The μ value was shown to increase with the incorporation of LP followed by a decrease when the LP dosage was beyond a certain value. For example, the increase of SBR dosage from 0 to 0.9% increased the μ value by 65%, but the further increasing SBR dosage to 1.8% led to 15% drop in the μ value. The use of LP had two opposite effects on μ: (1) the coalescence of LP polymer in transitional solution that can enhance μ [35]; and (2) the ball-bearing and air-entraining effect that can lower μ [61]. The latter played a dominate role to reduce the μ when the high LP dosage was added. Furthermore, the effect of LP on μ was lower than the VMA.

4.3. Structural build-up

Table 3 shows the variation of static yield stress (τ_s) with rest time for UHPC made with combinations of specialty admixtures and SP. The τ_s value was 175–360 Pa at 5 min, 275–920 Pa at 15 min, and 480–1865 Pa at 30 min. The coefficient of variation (COV) values were lower than 10%, indicating the proper reproductivity of the results. The τ_s value was shown to increase with the incorporation of VMAs and LPs, especially at the rest time of 15 and 30 min. For example, UHPC made with 0.0075% DG exhibited 285% higher τ_s value at 30 min compared to the reference mixture.

Table 3
Effect of competitive adsorption between specialty admixtures and SP on static yield stress of UHPC mortar with a constant mini-slump flow of 200 ± 10 mm.

Mixture	5 min	15 (min)	30 (min)
Ref	178	276	482
CE-0.25	177	404	615
CE-0.5	235	471	768
CE-1	314	598	1010
CE-1.5	296	506	937
WG-0.09	239	522	736
WG-0.18	321	847	1447
WG-0.27	316	752	1238
DG-0.0015	194	428	729
DG-0.003	359	821	1640
DG-0.0075	343	916	1863
DG-0.015	305	743	1201
SBR-0.45	185	380	719
SBR-0.9	184	429	768
SBR-1.8	198	434	900
AE-0.23	185	506	828
AE-0.45	203	495	1006
AE-0.9	205	504	992

Fig. 12 presents the influence of the competitive adsorption between specialty admixtures and SP on A_{sb} of UHPC mortar. In the case of VMA, the synergetic effect of DG and SP or WG and SP on enhancing structural build-up was higher compared to the addition of CE and SP. The incorporation of 0.0075% DG resulted in 410% increase in A_{sb} compared to the reference mortar. However, such enhancements were 135% for the mixture made with 1% CE. The structural build-up of UHPC mortar was shown to enhance by incorporating LP where the increasing amplitude was similar to the use of CE, and lower than that by the addition of WG and DG. The values of A_{sb} increased by 135% in mixture made with 1.8% SBR compared to the reference mixture. Such variations were 140% for the addition of 0.45% AE.

The relationship between zeta potential and A_{sb} was established in Fig. 13 to investigate the correlation between adsorption of specialty admixture and SP and the structural build-up of UHPC. In the case of WG, DG, SBR and AE, the lower value of zeta potential of slurry made with a certain specialty admixture referred to higher adsorption of such specialty admixture and lower adsorption of SP. For slurry made with CE, the reduction of the zeta potential reflected the increase of SP adsorption and decrease of CE adsorption. In general, the increased adsorption of all specialty admixtures enhanced the A_{sb} value. For example, the decrease of zeta potential from −20.5 to −22.5 mV referring to that the enhancement in WG adsorption led to 135% enhancement in A_{sb}. This can be attributed to the fact that the increased adsorption of the macromolecular polymers can strengthen the polymer network by combining the cement particles in the system [58,62]. On the other hand, the increase of SP adsorption led to a lower level of structural build-up. For instance, the A_{sb} value of slurry made with 0.1% DG reduced by 65% when the zeta potential increased from −10.5 to −9.0 mV. This result is consistent with the findings in previous studies [14,28] since the increase of SP adsorption can reduce the colloidal surface interaction and bridging effect of early age-hydration products.

A higher increase in structural build-up was observed by using DG compared to that of WG, although the relative adsorption content of DG was lower than that of WG given the lower zeta potential value. This demonstrates that the strength of the network is not solely dependent on adsorption of polymer onto the cement particles. The longer chain

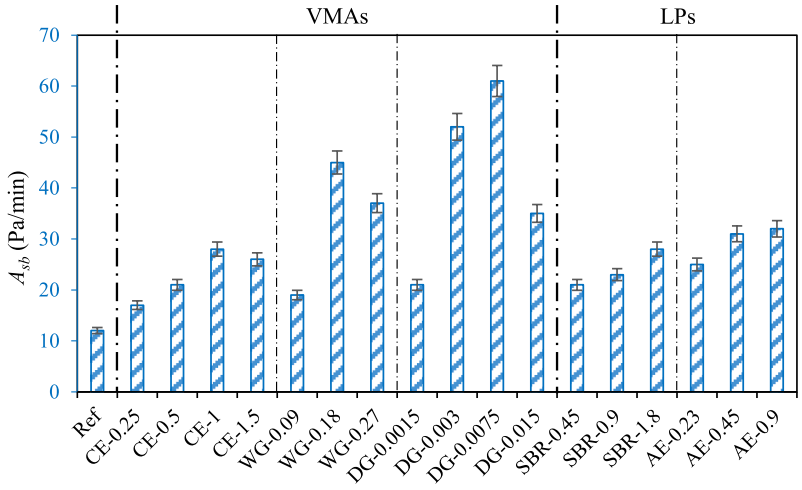

Fig. 12. Influence of competitive adsorption between specialty admixtures and SP on A_{sb} of UHPC mortar with a constant mini-slump flow of 200 ± 10 mm.

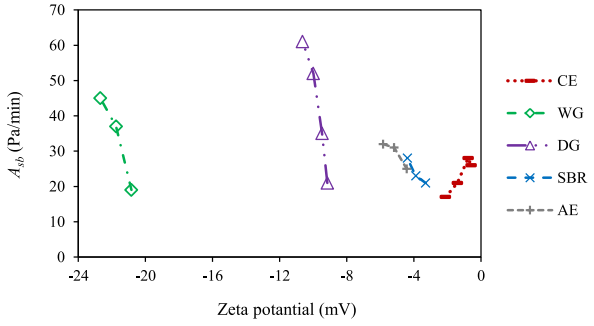

Fig. 13. Relationship between zeta potential and A_{sb}.

length of DG compared to WG can simultaneously adsorb onto several cement particles to enhance the bridging flocculation, which can result in a stronger physical polymer network and structural build-up of UHPC mortar [62]. In the case of CE, its low adsorption in the presence of SP led to most of CE remained in the interstitial pore solution, which resulted in limited effect on enhancing structural build-up.

The mechanism of LP affecting the structural build-up included two aspects. On one hand, the entanglement of long polymer chain can form a physical network in the interstitial pore solution [35]. Similar to CE, such effect cannot greatly increase the structural build-up. Furthermore, the ball-bearing effect induced by spherical LP and plasticizing effect due to presence of surfactants can reduce the particle flocculation [37,61], which can decrease the effect of entanglement of LP on increasing structural build-up.

It should be mentioned that the zeta potential test is a semi-quantitative method that can characterize the changing tendency of the competitive adsorption between specialty admixtures and SP. Such method cannot determine the adsorbed quantity of specialty admixtures and superplasticizer on the particles of cementitious materials.

4.4. Comparison of the dynamic and static yield stresses

The comparison of τ_s and τ_d values at various time can reflect the influence of the competitive adsorption between specialty admixtures and SP on the reversible component of structural build-up [63]. Table 4 shows the $\tau_s/\ \tau_d$ values of the UHPC mixtures made with VMA and LP at contents corresponding to the highest structural build-up. The $\tau_s/\ \tau_d$ value was shown to increase with time, which was 3.0–5.5, 3.5–10.0, and 4.5–15.0 at rest periods of 5, 15, and 30 min, respectively. This confirmed that the effect of competitive adsorption between SP and VMAs/LPs on enhancing structural build-up was mainly due to the increase in the reversible component of physical structuration instead of the chemical rigidification. UHPC made with WG and DG had the highest $\tau_s/\ \tau_d$ values at a given time, followed by UHPC prepared with CE and LP and the reference mixture. This was attributed to the effective adsorption of WG and DG in the presence of SP can greatly enhance the physical structuration since the polymer bridging flocculation and entanglement of polymers can combine the cement particles in the UHPC system together.

Table 4
Comparison between dynamic and static yield stress.

Mixture	$A_{\tau d}$ (Pa/min)	A_{sb} (Pa/min)	$\tau_s/\ \tau_d$		
			5 min	15 min	30 min
Ref	2.1	12.3	3.2	3.5	4.5
CE-1	1.5	27.8	5.2	7.3	10.2
WG-0.18	2.6	44.6	5.3	10.3	11.6
DG-0.0075	2.9	61.0	5.5	9.7	13.7
SBR-1.8	1.9	28.3	3.6	5.9	8.8
AE-0.45	1.8	31.5	4.1	7.5	10.8

The $A_{\tau d}$ values of the investigated mixtures are presented in Table 4. The COV values were lower than 10%, referring to the proper reproductivity of the results. UHPC prepared with WG and DG exhibited higher $A_{\tau d}$ values compared to the reference mixture due to the competitive adsorption between SP and WG/DG. The desorption of SP can enhance the early-age cement hydration (e.g., C_3A hydration), as proven by the results shown in Fig. 14(a) where the competitive adsorption between WG/DG and SP enhanced the cumulative heat at first hour. The non-adsorbed SP and VMA can also lead to depletion attractive forces to increase the τ_d [64–66]. On the other hand, UHPC made with LP exhibited a lower $A_{\tau d}$ values compared to the reference mixture. The possible reasons included the reduction in the early-age cement hydration by using LP (Fig. 14). Fig. 14(b) shows a linear relationship between $A_{\tau d}$ and cumulative heat at first hour where the increase of cumulative heat from 7 to 11 J increased the $A_{\tau d}$ from 1.5 to 2.9 Pa/min. This confirmed that the early-age hydration dominated the variation of irreversible component of the structural build-up. Furthermore, the $A_{\tau d}$ values were significantly lower than the A_{sb} values, indicating the impact of chemical rigidification on the structural build-up was limited due to the competitive adsorption between specialty admixtures and SP.

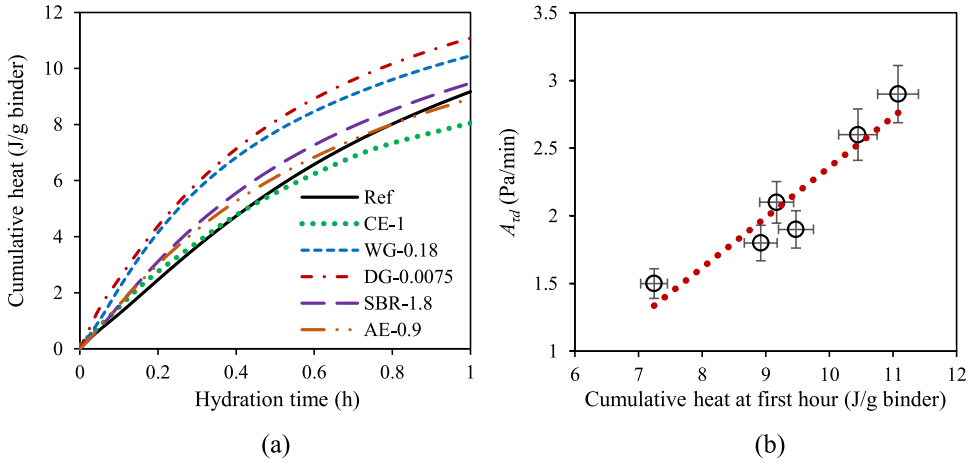

Fig. 14. Variations of: (a) cumulative heat with hydration time; and (b) $A_{\tau d}$ values with cumulative heat at first hour for UHPC mortar prepared with specialty admixtures and SP.

4.5. Compressive and pull-off strengths

The variation of compressive strength for non-fibrous UHPC mortar made with different combinations of specialty admixtures and SP is presented in Fig. 15. The compressive strength was 115 MPa when the reference mixture was subjected to 3-d moist curing followed by sealed condition. Such value was only 5 MPa less than that under continuous moist curing, reflecting the suitability of the proposed curing method. The compressive strength was shown to decrease by 2%–15% due to the use of combinations of VMAs and SP. For example, the increase of CE content from 0 to 1.5% reduced compressive strength from 115 to 97 MPa (15% decrease) at 28 d. Such decrease in strength can be in part due to the reduction of cement hydration due to the use of high SP content caused by competitive adsorption. Furthermore, the increase of plastic viscosity that can entrap additional air during mixing and placement [58,67]. On the other hand, the use of SBR and AE resulted in 8%–33% reduction in compressive strength compared to reference mixture when the same curing protocol was used. This can be attributed to the hydrophobic groups of the LP that can increase the entrained air in mortar mixtures as well as the reduction in cement hydration [35,37]. The combined effect of specialty admixtures and SP on entrapped air content and the capillary pore structure was discussed in Section 4.6 and 4.7, respectively. It should be mentioned that most of UHPC included 2% steel fibers; the increase of steel fiber contents from 0 to 2% can lead to 15%–40% increase in compressive strength of UHPC [68]. In addition to the mixtures made with 1.8% SBR or 0.9% AE, the compressive strength of the investigated mortar mixtures can be higher than 120 MPa after adding 2% steel fibers.

Fig. 16 shows failure modes of modified pull-off test using UHPC-NSM dogbone specimens based on the failure location. The first one was the interface failure, which occurred at the UHPC-NSM interface, as shown in Fig. 16(a). The area of UHPC at the interface was less than 10% of entire interface area. The second type was the NSM failure that took place within the NSM substrate, as presented in Fig. 16(b). This indicates that the bond strength was higher than the measured results. The last was the partial interface failure and partial UHPC failure, as shown in

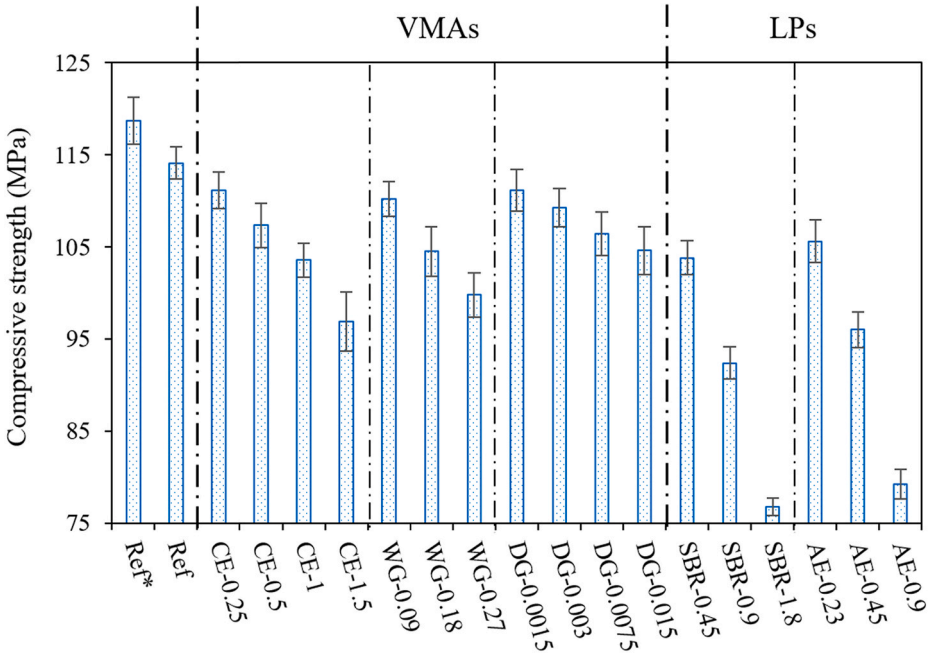

Fig. 15. Combined effect of specialty admixtures and SP on compressive strength of UHPC mortar at 28 d (* refers to continuous moist curing).

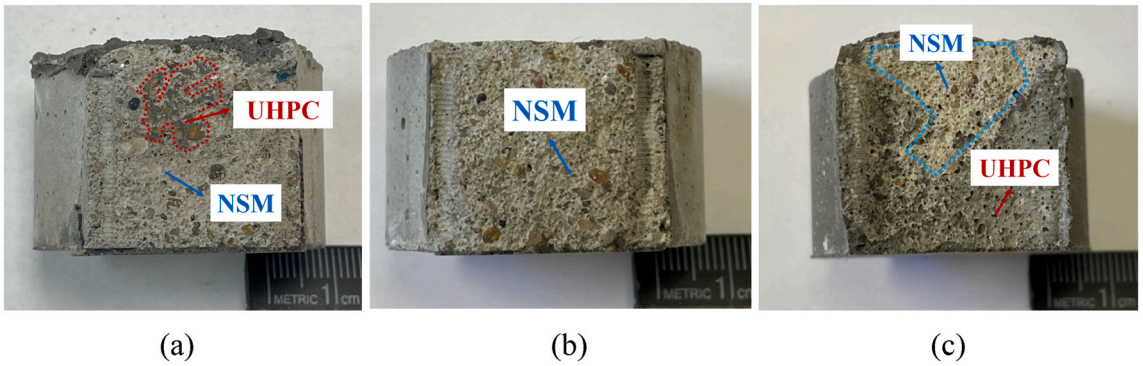

Fig. 16. Representative failure modes of modified pull-off test with failure plane located: (a) at interface (UHPC with high VMA content); (b) within NSM (typical for reference UHPC and UHPC with appropriate VMA or LP content); and (c) partial interface failure and partial NSM failure (typical for UHPC with high LP content).

Fig. 16(c). The ratio of UHPC failure area to entire failure area was greater than 40%.

Table 5 summarizes the variation of modified pull-off strength of the UHPC-NSM dogbone specimens. The COV values and failure modes were also reported. The pull-off failure occurred within NSM for reference mixture and mixtures made with low content of VMA and LP. The mean pull-off strengths of those mixtures were between 3.58 and 3.90 MPa where the COV values varied from 5.9% to 9.3%. Such strength values reflected the tensile pull-off strength of NSM.

The use of VMA at low content had a limited effect on the bond strength which, however, tended to decrease when incorporating VMA at a relatively high content. For example, the incorporation of 1.5% CE changed the failure location from NSM to interface, reflecting a reduction in bond strength. The use of LP at low dosage also secured the highest bond strength since the failure location was within the NSM material, despite the reduction in compressive strength. This can be attributed to the coalescence of polymers within the matrix and film formation phenomena at the interfaces that can enhance the bond strength between UHPC and NSM [33,37]. However, the pull-off strength reduced from 3.58-3.90 MPa to 2.60–2.75 MPa when 1.8% SBR and 0.9% AE were added. The failure mode changed from plane NSM failure to partial UHPC failure and partial interface failure. The drop in bond strength for UHPC containing high LP content can be attributed to the increased UHPC porosity that impaired the compressive and bond strengths, as shown in Fig. 16(c).

Table 5
Variations of modified pull-off strength of UHPC-NSM dogbone specimens.

Mixture	Pull-off strength (MPa)	COV (%)	Failure type
Ref[a]	3.74	5.9	NSM
Ref	3.81	8.3	NSM
CE-0.25	3.85	6.5	NSM
CE-0.5	3.66	6.2	NSM
CE-1	3.58	7.4	NSM
CE-1.5	3.42	5.9	Interface
WG-0.09	3.77	8.5	NSM
WG-0.18	3.72	7.9	NSM
WG-0.27	3.31	7.4	Interface
DG-0.0015	3.82	9.3	NSM
DG-0.003	3.87	6.8	NSM
DG-0.0075	3.73	8.8	NSM
DG-0.015	3.64	8.6	NSM
SBR-0.45	3.69	6.6	NSM
SBR-0.9	3.62	5.2	NSM
SBR-1.8	2.74	14.8	Interface & UHPC
AE-0.23	3.59	6.9	NSM
AE-0.45	3.73	7.3	NSM
AE-0.9	2.60	17.2	Interface & UHPC

[a] Refers to that the samples were subjected to the continuous moist curing.

4.6. Air void content

Fig. 17(a) presents the synergetic influence of specialty admixtures and SP on air voids with the diameter varying from 0.2 to 3.5 mm. The total volume of air void was between 0.5% and 3.0%. The combined use of VMAs and SP had a greater influence on the increase of entrapped air void compared to the incorporation of LPs, especially for CE and WG admixtures. The volume of air void was increased by 260% and 195% for the use of 1% CE and 0.18% WG, respectively. Such increase was limited to 40% with the use of 0.9% SBR, and 90% with the use of 0.45% AE. As earlier discussed, this was because the competitive adsorption between SP and WG/CE was more effective to increase plastic viscosity compared to LP (Fig. 11), leading to higher volume of entrapped air during mixing [58].

The combined influence of specialty admixtures and SP on the size distribution of air voids is shown in Fig. 17(b). The use of combinations of VMAs and SP increased the size of air void. For example, the maximum diameter of air void was less than 2.5 mm for the reference mixture; however, the WG-0.18 mixture had 0.25% air voids with diameter greater than 2.5 mm. Similar result was reported by Chen et al. [69] where the average void diameter was increased by 35% with the increase of the VMA content from 0.24% to 0.48%. Limited variation of air void with a diameter greater than 1 mm was found when SBR and AE were used. The air void with a diameter less than 1 mm was increased by 165% using SBR and 260% using AE. This was consistent with the findings in Ref. [35] where the use of LP increased the entrained air instead of the entrapped air due to the hydrophobic group of LP.

4.7. Pore structure

Fig. 18(a) presents the combined effect of specialty admixtures and SP on porosity of 28-d UHPC mortar where the pore diameter ranged between 5 nm and 200 μm. The reference mortar made without any specialty admixture exhibited the lowest porosity of 6.3%. The combined use of VMA and SP slightly increased the porosity; for example, the increase of WG content from 0 to 0.18% increased the total porosity from 6.3% to 7.5%. On the other hand, the porosity increased to 11% using 0.9% SBR and 10% using 0.45% AE. Such high porosity of UHPC made with LP was in a good agreement with the 8%–33% reduction of compressive strength compared to the reference mixture, as reported in Section 4.6.

The variation of pore size distribution for UHPC made with different combinations of specialty admixtures and SP is shown in Fig. 18(b). The pores were divided into macro pores (>5000 nm), capillary pores (10–5000 nm), and gel nano-pores (<10 nm) [70]. The capillary porosity was increased by 35% by using a combination of DG and SP. This was because the adsorption of VMA and SP onto the cement particles reduced the cement hydration [58,67]. The use of LPs significantly increased capillary pores compared to the reference UHPC prepared

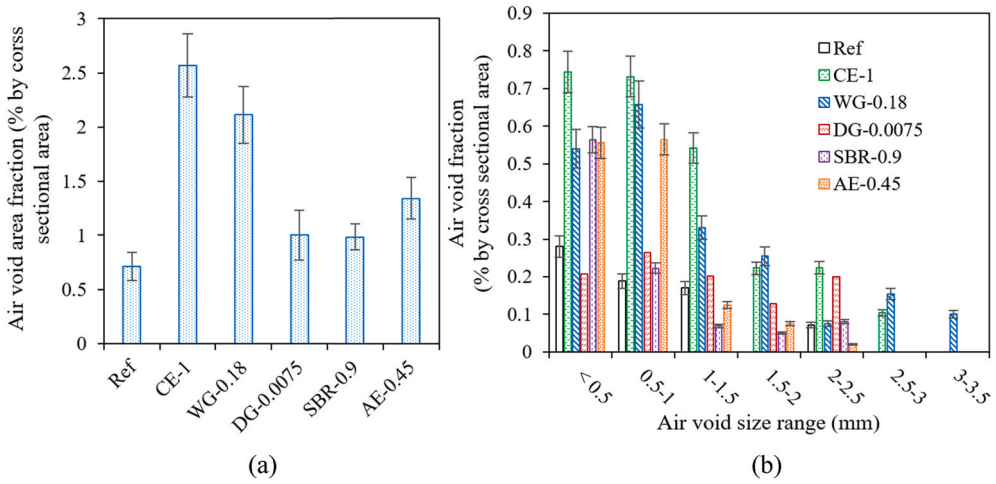

Fig. 17. Combined effect of specialty admixtures and SP on: (a) total volume; and (b) size distribution of entrapped air-void.

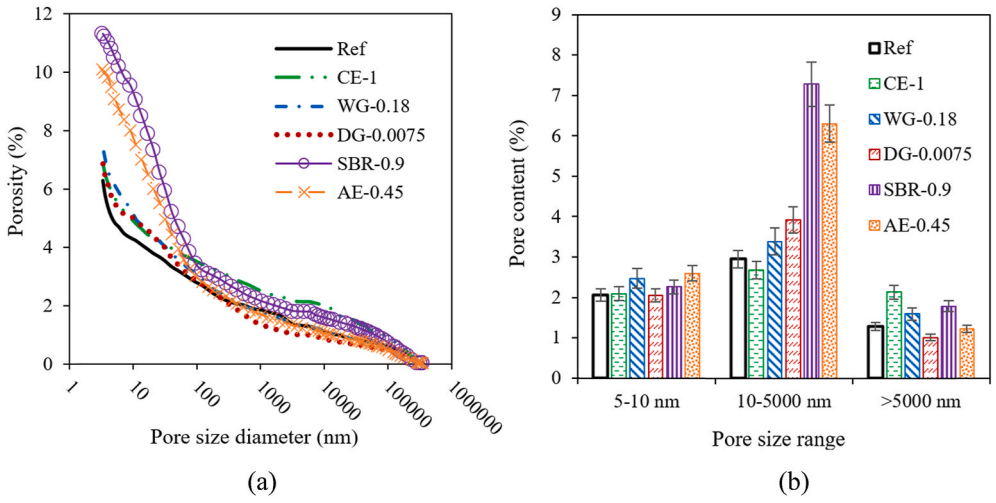

Fig. 18. Combined influence of specialty admixtures and SP on: (a) cumulative porosity; and (b) pore volume distribution.

with or without any VMAs. For example, the capillary pores were increased by 250% using 0.9% SBR. This can be attributed to the fact that the use of LPs can lead to a lower level of cement hydration given the LP film that can cover the cement particles to reduce their contact with water [35]. LP can also hinder the reaction of the ettringite with calcium aluminate hydrate and portlandite to generate the monosulfate [71]. Furthermore, the adsorption of LP onto the cement particles can decrease the nucleation site for the hydration products [72,73]. The other possible reason is that the hydrophobic groups of LP can introduce and stabilize the fine pores [33,35].

5. Conclusion

This study investigates the competitive adsorption between specialty admixtures and SP and its effect on the dynamic yield stress, plastic viscosity, and structural build-up of UHPC mortar mixtures made with mini-slump flow of 200 ± 10 mm. The reversible part of structural build-up was evaluated by comparing the dynamic and static yield stress that were measured using re-agitated and undisturbed samples, respectively. The influence of competitive adsorption between specialty admixtures and SP on early-age cement hydration was determined to understand the irreversible part of structural build-up (i.e., the increase of dynamic yield stress with time). The entrapped air and porosity were evaluated to elucidate the synergetic impact of specialty admixtures and SP on compressive and pull-off strengths. Based on the above experimental investigations, the following conclusions can be drawn:

(1) The use of anionic WG and DG at moderate content exhibited high competitive adsorption with SP, which greatly enhanced the A_{sb} by 275%–450%, respectively, despite the 55%–135% increase in SP demand to maintain the initial fluidity. This was mainly attributed to the fact that the adsorbed WG and DG combined the cement particles in the system to strengthen the flocculation. Furthermore, the effect of WG and DG on enhancing structural build-up became lower with the incorporation of WG and DG at high content since part of WG and DG was desorbed by SP after the surface coverage of cement particle was saturated.
(2) The increased SP demand with the incorporation of non-ionic CE led to desorption of CE and resulting limited enhancement in A_{sb} compared to the reference mixture. In spite of the limited variation of SP content, the incorporation of LPs had an insignificant impact on enhancing structural build-up compared to the use of DG and WG given their low adsorption in the presence of the SP. This demonstrated that the entanglement of polymers remaining in the interstitial pore solution had an inferior contribution on enhancing structural build-up.
(3) The high competitive adsorption between WG/DG and SP that decreased the effect of SP on the cement hydration at first hour

led to approximately 30% increase in A_{rd}, despite the delay of the onset of acceleration period due to the higher SP demand. The use of CE and LP was shown to slightly reduce the cement hydration at first hour and resulting 10%–25% lower A_{rd}. Furthermore, the A_{rd} values of 1.5–2.9 Pa/min were significantly lower than A_{sb} values of 12–61 Pa/min, indicating that competitive adsorption between specialty admixtures and SP mainly influenced the reversible part of structural build-up in the first hour.

(4) The combined use of WG and SP was most effective to increase plastic viscosity without influencing the dynamic yield stress, followed by CE and DG. This can be associated with the moderate molecular wight of WG and effective competitive adsorption between WG and SP. The addition of DG with high molecular weight led to a significant increase of SP demand to desorb DG from multiple cement particles, which restrained the increase of plastic viscosity. The high amount of CE remaining in the interstitial pore solution given the low adsorption of CE in the presence of SP can result in the hydrodynamic lubrication, which can lower the effect of CE on enhancing plastic viscosity. Moreover, the impact of LP on plastic viscosity was limited due to the ball-bearing and air-entraining effect that can reduce the influence of LP coalescence on increasing plastic viscosity.

(5) The combined use of VMA and SP had a limited effect on UHPC-NSM bond strength, whereas the compressive strength was reduced by 5%–15%. The latter was associated with the 80%–260% increase of entrapped air given the higher plastic viscosity. Furthermore, the combined incorporation of VMAs and SP slightly increased the total porosity from 6.3% to 7.5%. The use of LP at appropriate dosage can secure high UHPC-NSM bond strength. However, the addition of LP at high dosage increased volume of capillary pore by 70%, which decreased compressive strength up to 35%. Such substantial increase of capillary porosity also led to a loose interface and lower UHPC-NSM bond strength.

Declaration of competing interest

The authors declare that they have no known competing financial interests or personal relationship that could have appeared to influence the work reported in this paper.

Data availability

Data will be made available on request.

Acknowledgement

The authors acknowledge the financial support provided by the Missouri DOT [Grant Number: TR2021-21]. This research was conducted at the Advanced Construction and Material Laboratory (ACML) of the Center for Infrastructure Engineering Studies (CIES) at Missouri S&T.

References

[1] Q. Song, R. Yu, Z. Shui, S. Rao, D. Fan, X. Gao, Macro/micro characteristics variation of ultra-high performance fibre reinforced concrete (UHPFRC) subjected to critical marine environments, Construct. Build. Mater. 256 (2020), 119458.
[2] L. Teng, H. Huang, J. Du, K.H. Khayat, Prediction of fiber orientation and flexural performance of UHPC based on suspending mortar rheology and casting method, Cem. Concr. Compos. (2021), 104142.
[3] J.H. Lee, D.Y. Yoo, Full-scale pumping tests of low-viscosity ultra-high-strength concrete, J. Build. Eng. 43 (2021), 102616.
[4] K.H. Khayat, W. Meng, K. Vallurupalli, L. Teng, Rheological properties of ultra-high-performance concrete — an overview, Cement Concr. Res. 124 (2019), 105828.
[5] L. Teng, M. Valipour, K.H. Khayat, Design and performance of low shrinkage UHPC for thin bonded bridge deck overlay, Cem. Concr. Compos. (2021), 103953.
[6] L. Teng, K.H. Khayat, Effect of overlay thickness, fiber volume, and shrinkage mitigation on flexural behavior of thin bonded ultra-high-performance concrete overlay slab, Cem. Concr. Compos. (2022), 104752.
[7] Z. Xu, Z. Li, Numerical method for predicting flow and segregation behaviors of fresh concrete, Cem. Concr. Compos. 123 (2021), 104150.
[8] S. Sritharan, G. Doiron, D. Bierwagen, B. Keierleber, A. Abu-Hawash, First application of UHPC bridge deck overlay in North America, Transport. Res. Rec. 2672 (2018) 40–47.
[9] J.J. Assaad, K.H. Khayat, Form pressure characteristics of self-consolidating concrete used in repair, Cem. Concr. Compos. 122 (2021), 104118.
[10] A.F. Omran, K.H. Khayat, Choice of thixotropic index to evaluate formwork pressure characteristics of self-consolidating concrete, Cement Concr. Res. 63 (2014) 89–97.
[11] J.J. Assaad, Correlating thixotropy of self-consolidating concrete to stability, formwork pressure, and multilayer casting, J. Mater. Civ. Eng. 28 (2016), 04016107.
[12] K.H. Khayat, J.J. Assaad, Use of thixotropy-enhancing agent to reduce formwork pressure exerted by self-consolidating concrete, ACI Mater. J. 105 (2008) 88–96.
[13] D. Jiao, R. De Schryver, C. Shi, G. De Schutter, Thixotropic structural build-up of cement-based materials: a state-of-the-art review, Cem. Concr. Compos. 122 (2021), 104152.
[14] D. Lowke, Thixotropy of SCC—a model describing the effect of particle packing and superplasticizer adsorption on thixotropic structural build-up of the mortar phase based on interparticle interactions, Cement Concr. Res. 104 (2018) 94–104.
[15] N. Roussel, A. Lemaître, R.J. Flatt, P. Coussot, Steady state flow of cement suspensions: a micromechanical state of the art, Cement Concr. Res. 40 (2010) 77–84.
[16] R.J. Flatt, P. Bowen, Yodel: a yield stress model for suspensions, J. Am. Ceram. Soc. 89 (2006) 1244–1256.
[17] R.J. Flatt, P. Bowen, Yield stress of multimodal powder suspensions: an extension of the YODEL (Yield Stress mODEL), J. Am. Ceram. Soc. 90 (2007) 1038–1044.
[18] N. Roussel, G. Ovarlez, S. Garrault, C. Brumaud, The origins of thixotropy of fresh cement pastes, Cement Concr. Res. 42 (2012) 148–157.
[19] Q. Yuan, D. Zhou, K.H. Khayat, D. Feys, C. Shi, On the measurement of evolution of structural build-up of cement paste with time by static yield stress test vs. small amplitude oscillatory shear test, Cement Concr. Res. 99 (2017) 183–189.
[20] Y. Zhang, X. Kong, Correlations of the dispersing capability of NSF and PCE types of superplasticizer and their impacts on cement hydration with the adsorption in fresh cement pastes, Cement Concr. Res. 69 (2015) 1–9.
[21] J. Zhu, J. Liu, K.H. Khayat, X. Shu, Z. Li, Effect of particle contact and high-range water-reducing admixture adsorption on rheology of cement paste, ACI Mater. J. 118 (2021) 341–351.
[22] K.H. Khayat, J.J. Assaad, Effect of w/cm and high-range water-reducing admixture on formwork pressure and thixotropy of self-consolidating concrete, ACI Mater. J. 103 (2006) 186–193.
[23] I. Navarrete, Y. Kurama, N. Escalona, M. Lopez, Impact of physical and physicochemical properties of supplementary cementitious materials on structural build-up of cement-based pastes, Cement Concr. Res. 130 (2020), 105994.
[24] R. Saleh Ahari, T.K. Erdem, K. Ramyar, Time-dependent rheological characteristics of self-consolidating concrete containing various mineral admixtures, Construct. Build. Mater. 88 (2015) 134–142.
[25] Y. Qian, S. Kawashima, Use of creep recovery protocol to measure static yield stress and structural rebuilding of fresh cement pastes, Cement Concr. Res. 90 (2016) 73–79.
[26] Y. Qian, G. De Schutter, Enhancing thixotropy of fresh cement pastes with nanoclay in presence of polycarboxylate ether superplasticizer (PCE), Cem, Concr. Res. 111 (2018) 15–22.
[27] R.J. Flatt, Y.F. Houst, A simplified view on chemical effects perturbing the action of superplasticizers, Cement Concr. Res. 31 (2001) 1169–1176.
[28] Y. Qian, Effect of polycarboxylate ether (PCE) superplasticizer on thixotropic structural build-up of fresh cement pastes over time, Construct. Build. Mater. 291 (2021), 123241.
[29] Y. Qian, K. Lesage, K. El Cheikh, G. De Schutter, Effect of polycarboxylate ether superplasticizer (PCE) on dynamic yield stress, thixotropy and flocculation state of fresh cement pastes in consideration of the Critical Micelle Concentration (CMC), Cement Concr. Res. 107 (2018) 75–84.
[30] L. Teng, J. Zhu, K.H. Khayat, J. Liu, Effect of welan gum and nanoclay on thixotropy of UHPC, Cement Concr. Res. 138 (2020), 106238.
[31] S. Ma, Y. Qian, S. Kawashima, Experimental and modeling study on the non-linear structural build-up of fresh cement pastes incorporating viscosity modifying admixtures, Cement Concr. Res. 108 (2018) 1–9.
[32] J. Cui, Z. He, G. Zhang, X. Cai, Rheological properties of sprayable ultra-high performance concrete with different viscosity-enhancing agents, Construct. Build. Mater. 321 (2022), 126154.
[33] J.J. Assaad, K.H. Khayat, Rheology of fiber-reinforced high-strength grout modified with polymer latexes, ACI Mater. J. 118 (2021).
[34] C.A. Issa, J.J. Assaad, Stability and bond properties of polymer-modified self-consolidating concrete for repair applications, Mater. Struct. Constr. 50 (2017) 1–16.
[35] K. Sun, S. Wang, L. Zeng, X. Peng, Effect of styrene-butadiene rubber latex on the rheological behavior and pore structure of cement paste, Compos. B Eng. 163 (2019) 282–289.
[36] Z.B. Haber, J.F. Munoz, I. De la Varga, B.A. Graybeal, Bond characterization of UHPC overlays for concrete bridge decks: Laboratory and field testing, Construct. Build. Mater. 190 (2018) 1056–1068.

[37] J.J. Assaad, Development and use of polymer-modified cement for adhesive and repair applications, Construct. Build. Mater. 163 (2018) 139–148.
[38] F. El Sakka, J.J. Assaad, F.R. Hamzeh, C. Nakhoul, Thixotropy and interfacial bond strengths of polymer-modified printed mortars, Mater. Struct. Constr. 52 (2019) 1–17.
[39] V. Kaur, M.B. Bera, P.S. Panesar, H. Kumar, J.F. Kennedy, Welan gum: microbial production, characterization, and applications, Int. J. Biol. Macromol. 65 (2014) 454–461.
[40] H. Bessaies-Bey, K.H. Khayat, M. Palacios, W. Schmidt, N. Roussel, Viscosity modifying agents: key components of advanced cement-based materials with adapted rheology, Cement Concr. Res. 152 (2022), 106646.
[41] W. Meng, M. Valipour, K.H. Khayat, Optimization and performance of cost-effective ultra-high performance concrete, Mater. Struct. Constr. 50 (2017) 1–16.
[42] O.H. Wallevik, D. Feys, J.E. Wallevik, K.H. Khayat, Avoiding inaccurate interpretations of rheological measurements for cement-based materials, Cement Concr. Res. 78 (2015) 100–109.
[43] Y. Liu, C. Shi, Q. Yuan, X. An, L. Zhu, B. Wu, The rotation speed-torque transformation equation of the Robertson-Stiff model in wide gap coaxial cylinders rheometer and its applications for fresh concrete, Cem. Concr. Compos. 107 (2020), 103511.
[44] A. Arunothayan, B. Nematollahi, R. Ranade, K.H. Khayat, H.G. Sanjayan, Digital fabrication of eco-friendly ultra-high performance concrete, Cem. Concr. Compos. 125 (2022), 104281.
[45] K.H. Khayat, Performance of Synthetic Fiber-reinforced Concrete with Adapted Rheology, Res. on Concr. Applica. for Sustain. Trans (2020).
[46] J. Zhu, J. Liu, K.H. Khayat, X. Shu, Q. Ran, Z. Li, Mechanisms affecting viscosity of cement paste made with microfines of manufactured sand, Cement Concr. Res. 156 (2022), 106757.
[47] J. Chen, M. Qiao, N. Gao, J. Wu, G. Shan, B. Zhu, Q. Ran, Acrylate based post-acting polymers as novel viscosity modifying admixtures for concrete, Construct. Build. Mater. 312 (2021), 125414.
[48] M. Qiao, J. Chen, N. Gao, G. Shan, J. Wu, B. Zhu, Q. Ran, Effects of adsorption group and molecular weight of viscosity-modifying admixtures on the properties of cement paste, J. Mater. Civ. Eng. 34 (2022), 04022148.
[49] S. Sha, Y. Zhang, Y. Ma, Y. Liu, C. Shi, Effect of molecular structure of maleic anhydride, fumaric acid – isopentenyl polyoxyethylene ether based polycarboxylate superplasticizer on its properties in cement pastes, Construct. Build. Mater. 308 (2021), 125143.
[50] B. Ma, C. Li, Y. Lv, H. Tan, H. Wang, H. Qi, X. Liu, Q. Yang, P. Chen, Preparation for polyacrylic acid modified by ester group in side chain and its application as viscosity enhancing agent in polycarboxylate superplasticizer system, Construct. Build. Mater. 233 (2020), 117272.
[51] P.P. Li, Q.L. Yu, H.J.H. Brouwers, Effect of PCE-type superplasticizer on early-age behaviour of ultra-high performance concrete (UHPC), Construct. Build. Mater. 153 (2017) 740–750.
[52] D. Lowke, C. Gehlen, The zeta potential of cement and additions in cementitious suspensions with high solid fraction, Cement Concr. Res. 95 (2017) 195–204.
[53] R. Sposito, M. Maier, N. Beuntner, K.C. Thienel, Evaluation of zeta potential of calcined clays and time-dependent flowability of blended cements with customized polycarboxylate-based superplasticizers, Construct. Build. Mater. 308 (2021), 125061.
[54] M. Palacios, R.J. Flatt, F. Puertas, A. Sanchez-Herencia, Compatibility between polycarboxylate and viscosity-modifying admixtures in cement pastes, ACI Spec. Publ. 288 (2012) 29–42.
[55] T. Hurnaus, J. Plank, Adsorption of non-ionic cellulose ethers on cement revisited, Construct. Build. Mater. 195 (2019) 441–449.
[56] C. Brumaud, H. Bessaies-Bey, C. Mohler, R. Baumann, M. Schmitz, M. Radler, N. Roussel, Cellulose ethers and water retention, Cement Concr. Res. 53 (2013) 176–184.
[57] H. Bessaies-Bey, R. Baumann, M. Schmitz, M. Radler, N. Roussel, Organic admixtures and cement particles: competitive adsorption and its macroscopic rheological consequences, Cement Concr. Res. 80 (2016) 1–9.
[58] L. Teng, W. Meng, K.H. Khayat, Rheology control of ultra-high-performance concrete made with different fiber contents, Cement Concr. Res. 138 (2020), 106222.
[59] N. Roussel, P. Coussot, “Fifty-cent rheometer” for yield stress measurements: from slump to spreading flow, J. Rheol. 49 (2005) 705.
[60] J. Hot, H. Bessaies-Bey, C. Brumaud, R.M. Duc, C. Castella, N. Roussel, Adsorbing polymers and viscosity of cement pastes, Cement Concr. Res. 63 (2014) 12–19.
[61] C. Zhang, X. Kong, J. Yu, D. Jansen, J. Pakusch, S. Wang, Correlation between the adsorption behavior of colloidal polymer particles and the yield stress of fresh cement pastes, Cement Concr. Res. 152 (2022), 106668.
[62] N. Roussel, Understanding the Rheology of Concrete, Elsevier, 2011.
[63] K. Zhang, A. Mezhov, W. Schmidt, Chemical and thixotropic contribution to the structural build-up of cementitious materials, Construct. Build. Mater. 345 (2022), 128307.
[64] H. Bessaies-Bey, M. Palacios, E. Pustovgar, M. Hanafi, R. Baumann, R.J. Flatt, N. Roussel, Non-adsorbing polymers and yield stress of cement paste: effect of depletion forces, Cement Concr. Res. 111 (2018) 209–217.
[65] N. Roussel, H. Bessaies-Bey, S. Kawashima, D. Marchon, K. Vasilic, R. Wolfs, Recent advances on yield stress and elasticity of fresh cement-based materials, Cement Concr. Res. 124 (2019), 105798.
[66] J. Cheung, A. Jeknavorian, L. Roberts, D. Silva, Impact of admixtures on the hydration kinetics of Portland cement, Cement Concr. Res. 41 (2011) 1289–1309.
[67] W. Meng, K.H. Khayat, Improving flexural performance of ultra-high-performance concrete by rheology control of suspending mortar, Compos. B Eng. 117 (2017) 26–34.
[68] Z. Wu, C. Shi, W. He, L. Wu, Effects of steel fiber content and shape on mechanical properties of ultra high performance concrete, Construct. Build. Mater. 103 (2016) 8–14.
[69] Y. Chen, S.C. Figueiredo, Z. Li, Z. Chang, K. Jansen, O. Copuroglu, E. Schlangen, Improving printability of limestone-calcined clay-based cementitious materials by using viscosity-modifying admixture, Cement Concr. Res. 132 (2020), 106040.
[70] L. Teng, A. Addai-Nimoh, K.H. Khayat, Effect of lightweight sand and shrinkage reducing admixture on structural build-up and mechanical performance of UHPC, J. Build. Eng. 68 (2023), 106144.
[71] D. Cheng, X. Li, X. Gao, X. Fan, R. Zhao, T. Yang, Influence of polymer latexs on the properties of high performance cement-based materials, Crystals 12 (2022) 789.
[72] X. Kong, S. Emmerling, J. Pakusch, M. Rueckel, J. Nieberle, Retardation effect of styrene-acrylate copolymer latexes on cement hydration, Cement Concr. Res. 75 (2015) 23–41.
[73] M. Wang, R. Wang, H. Yao, S. Farhan, S. Zheng, Z. Wang, C. Du, H. Jiang, Research on the mechanism of polymer latex modified cement, Construct. Build. Mater. 111 (2016) 710–718.